CardioVascular and Interventional Radiology

Published Online: 6 May 2004

Cardiovasc Intervent Radiol (2004) 27:370–373
DOI: 10.1007/s00270-003-0079-9

Feasibility of Respiratory Triggering for MR-Guided Microwave Ablation of Liver Tumors Under General Anesthesia

Shigehiro Morikawa,[1] Toshiro Inubushi,[1] Yoshimasa Kurumi,[2] Shigeyuki Naka,[2] Koichiro Sato,[2] Koichi Demura,[2] Tohru Tani,[2] Hasnine A Haque[3]

[1]Molecular Neuroscience Research Center, Shiga University of Medical Science, Seta Tsukinowa-cho, Ohtsu, Shiga, 520-2192, Japan
[2]Department of Surgery, Shiga University of Medical Science, Seta Tsukinowa-cho, Ohtsu, Shiga 520-2192, Japan
[3]GE-Yokogawa Medical Systems, Asahigaoka, Hino, Tokyo 191-8503, Japan

Abstract

We obtained clear and reproducible MR fluoroscopic images and temperature maps for MR image-guided microwave ablation of liver tumors under general anesthesia without suspending the artificial ventilation. Respiratory information was directly obtained from air-way pressure without a sensor on the chest wall. The trigger signal started scanning of one whole image with a spoiled gradient echo sequence. The delay time before the start of scanning was adjusted to acquire the data corresponding to the k-space center at the maximal expiratory phase. The triggered images were apparently clearer than the nontriggered ones and the location of the liver was consistent, which made targeting of the tumor easy. MR temperature images, which were highly susceptible to the movement of the liver, during microwave ablation using a proton resonance frequency method, could be obtained without suspending the artificial ventilation. Respiratory triggering technique was found to be useful for MR fluoroscopic images and MR temperature monitoring in MR-guided microwave ablation of liver tumors under general anesthesia.

Key words: MR-guided intervention—Respiratory triggering—Microwave ablation—MR temperature mapping—Liver tumor

Open configuration MR scanners have successfully improved accessibility to patients and have permitted new minimally invasive procedures under the guidance of MR images [1]. In Japan, microwave thermocoagulation therapy, operated at 2.45 GHz, has been developed for liver surgery for more than 20 years [2]. Initially, it was used for hemostasis and tissue destruction under laparotomy [3]. It has also been used as an interventional procedure for liver tumors under ultrasound or laparoscopic guidance [4, 5]. One advantage of microwave ablation under the MR environments is that the microwave coagulator does not interfere with MR images even during ablation [6]. We have reported our experience in MR-guided microwave ablation of liver tumors with an open configuration MR system [7, 8]. MR images could be used not only for image navigation during the percutaneous puncture of liver tumors, but also for temperature monitoring during microwave ablation [9, 10]. In this procedure, general anesthesia was utilized because repeated punctures and ablations were generally required.

MR images of the liver for diagnosis are usually acquired under voluntary breath holding, otherwise they would be blurred because of respiratory motion. In interventional use, however, near-real-time MR images are acquired continuously every 2–3 seconds during targeting and puncture. In the critical period of puncture, artificial ventilation is suspended by the anesthesiologist, but it is not practical to apply respiratory suspension so frequently. Temperature monitoring using the proton resonance frequency method is highly susceptible to the movement of the liver. Because temperature change is calculated using subtraction techniques between objective and reference images on a pixel-to-pixel basis, dislocation of a pixel may cause errors in calculated temperature change. For the acquisition of temperature data, respiration has to be suspended to eliminate the movement, but some periods for hyperventilation must be interleaved during the ablation for several minutes. Conventional respiratory triggering [11], which controls each RF pulse, did not fit the rapid acquisition for near-real-time MR images and temperature monitoring. To solve such problems, we have

Correspondence to: Shigehiro Morikawa; *email:* morikawa@belle.shiga-med.ac.jp

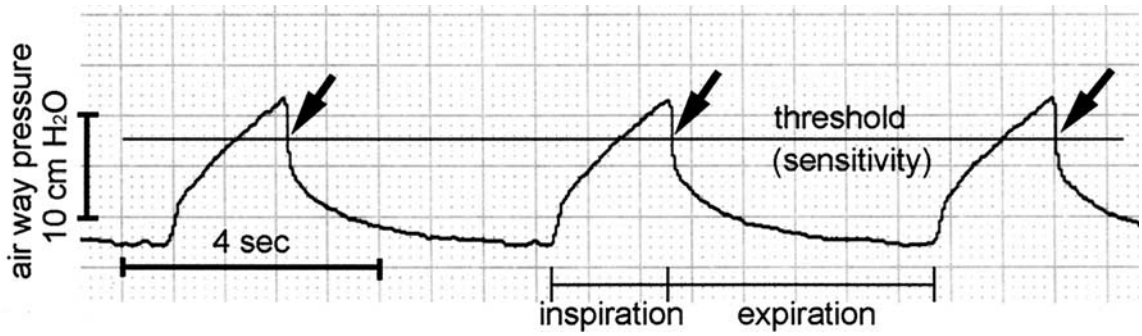

Fig. 1. Representative airway pressure pattern. The airway pressure gradually increases in the inspiratory phase and rapidly decreases from the maximal level in the expiratory phase. The sensitivity for the trigger circuit could be changed by adjusting the threshold level. The time points, when the pressure dropped below this level (arrows), were detected.

developed a suitable respiratory triggering technique for this procedure.

Materials and Methods

The Ethics Committee of Shiga University of Medical Science approved this study. The procedure and any possible complications related to this type of therapy were explained to each patient, and signed informed consent was obtained from the subjects. All MR data were collected on an open configuration 0.5 T superconducting SIGNA SP/i system (GE Medical Systems, Milwaukee, WI). A Microtaze®, microwave coagulator (OT-110M, Azwell, Osaka, Japan) was used as the heating device. General anesthesia was performed using an MR-compatible Excel 210 MRI anesthesia machine, AS/3CM monitor (Datex Ohmeda, Helsinki, Finland) and VentiPac 5 MRI ventilator (Pneupac, Luton, UK). The respiratory rate was set at 10–14 times per minute depending on the patient's condition. The durations of the inspiratory and expiratory phases were usually set at a ratio of 1 : 2. The airway pressure of the patient was monitored from an analog output of the AS/3CM monitor. When artificial ventilation changed from the inspiratory phase to the expiratory phase, the airway pressure rapidly decreased from the maximal level (Fig. 1). To pick up this time point, a trigger circuit was custom-made. The sensitivity could be changed by adjusting the threshold level. The time points when the pressure dropped below this level were detected (Fig. 1, arrows). The delay time before generating a trigger pulse could be controlled at a range of 80–5000 ms with this circuit box without changing the MR acquisition parameters. The trigger pulse was transferred from the circuit box in the magnet room to the MR system console with a coaxial cable through a penetration panel. This trigger pulse initiated the acquisition of an image scan for 2–4 seconds with a spoiled gradient echo (SPGR) sequence.

Near-real-time MR images were acquired with 14 ms/3.7 ms (TR/TE) and 30 x 30 cm^2 FOV, and temperature increase maps were acquired with 33 ms/13 ms (TR/TE) and 24 x 24 cm^2 FOV with 256 x 128 resolutions. Temperature changes from the baseline data were calculated using the proton resonance frequency method [9, 10] with a thermal coefficient value of -0.01 ppm/°C. This respiratory triggering technique was utilized in some parts of the procedures in 33 patients with microwave thermocoagulation therapy of liver tumors. In 3 cases, 30 consecutive near-real-time images with and without respiratory triggering were acquired in a fixed sagittal plane for the evaluation of the top position of the diaphragm.

Various delay times for the acquisition were examined with various respiratory rates. Under ventilation at a rate of 10 times/minute (2-second inspiration and 4-second expiration), near-real-time images were clear with 500 ms or 1000 ms delay time, but some of them were blurred with 1500 ms delay time. Therefore, the delay time was set at 500 ms for near-real-time images. For temperature increase maps, which required 4.2 seconds for one image, the delay time was set at 100 ms. An MR-compatible needle type electrode (1.6 mm in diameter, Azwell, Osaka, Japan) was inserted into the tumor through the outer sheath of a percutaneously punctured 14G MR-compatible needle (Daum, Schwerin, Germany). Three-minute ablations, which caused an ellipsoid coagulation area 20 mm in diameter and 30 mm in length along the electrode, were repeated depending on the size of the tumor.

Results

The trigger box did not interfere with the MR images by electromagnetic noises. Serial near-real-time MR images of the liver in the sagittal plane without and with respiratory triggering are shown in Figure 2. In order to easily compare the top positions of the diaphragm, white lines were added at their highest locations in individual series. Without respiratory triggering, a 20-pixel difference in the top position of the diaphragm, which corresponded to 23 mm, was observed within the 6 serial images of this case. In the images at a relatively high position of the diaphragm (expiratory phase), the tumor was clearly visualized, but in those images at relatively low positions (inspiratory phase, 1st, 3rd and 6th images), the target was not very clear and the contour of the liver was blurred. On the other hand, with respiratory triggering, the positions of the diaphragm were consistent and the tumor was clearly visualized in all 6 images. In the other 2 cases, the dispersion of the top position of the diaphragm without respiratory triggering was 17.6 mm and 15.5 mm, respectively. Figure 3 shows the temperature increase during 3-minute microwave ablation with respiratory triggering un-

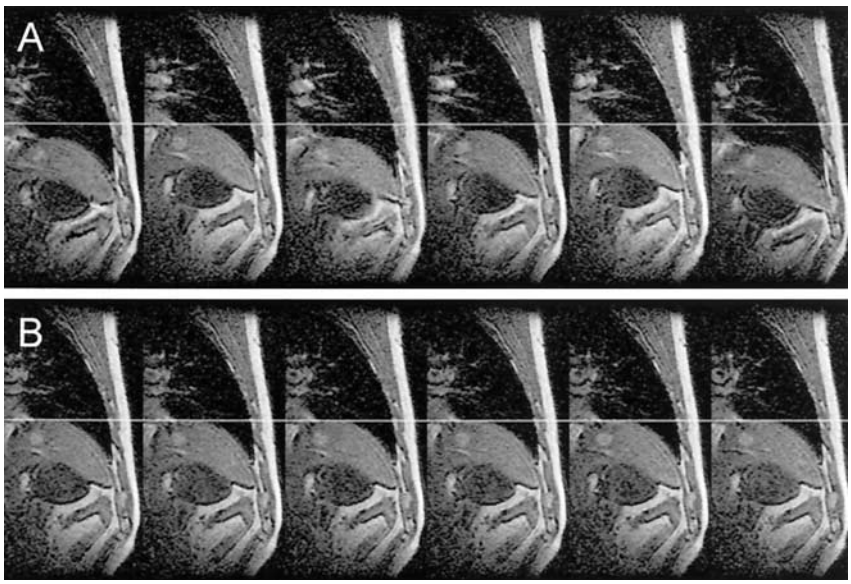

Fig. 2. Six serial MR images of the liver in the sagittal plane without **(A)** and with **(B)** respiratory triggering acquired with a SPGR (14/3.7: TR/TE). The acquisition time for one image was 1.8 s. The images without triggering **(A)** were acquired consecutively under the artificial ventilation. To indicate the top positions of the diaphragm, white lines were added at their highest locations in individual series. The tumor was visualized with high intensities.

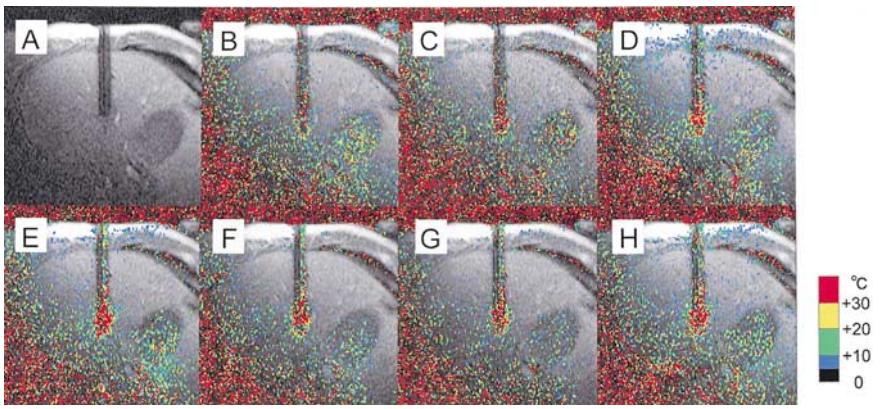

Fig. 3. MR temperature increase maps during 3-minute microwave ablation of a liver tumor. Temperature increases are shown with a color scale on the right side. **(A)** Magnitude, **(B)** 15-second, **(C)** 30-second, **(D)** 60-second, **(E)** 90-second, **(F)** 120-second, **(G)** 150-second and **(H)** 180-second microwave ablation. Around the electrode tip, temperature increase was clearly observed. In the background and in parts, where the MR signal levels were low, considerable scattering of the calculated temperature was observed.

der artificial ventilation of general anesthesia. The obtained data were compatible to those under respiratory suspension.

Discussion

Respiratory triggering is the simplest way to prevent MR image degradation caused by movement. Reordering of phase encoding [12], navigation echo [13] and post-processing [14] have also been utilized for this purpose, but these techniques are not practical during the interventional procedure, in which rapid image acquisition is required. Respiratory triggering is not a new technique, but conventional triggering [11] could not be applied for near-real-time MR images and temperature monitoring, which were taken continuously every 2 and 4 seconds, respectively. Meanwhile, the respiration of the patient during the procedure was generally maintained by a ventilator at a rate of 10–14 times/minute, which was more consistent and reproducible than the spontaneous ventilation. Therefore, one MR image was taken in one respiratory cycle at the same respiratory phase.

Since the SPGR images were acquired with sequential phase-encoding steps, we intended to measure the data of the k-space center at the expiratory phase, when the respiratory movement was minimal. Information regarding the respiration of the patients under general anesthesia could be easily monitored without employing any additional sensors on the chest wall, which might sometimes disturb procedures for the liver. Monitoring of CO_2 concentration was one candidate, but sampling of gas through a long tube caused a long delay time. We took notice of the airway pressure, which clearly showed the turning point from the inspiratory to the expiratory phases without sampling delay. The function of the trigger box to control the delay time was quite useful, because changing the parameter of the MR scanner was a time-consuming process. The optimal delay times of 500 ms and 1000 ms for the near-real-time MR images under a 6-second respiratory cycle were shorter than we had anticipated.

The sensor of the airway pressure was connected with the ventilation circuit close to the patient via a 5-meter long

tube. Substantial time delay seems to have occurred for the detection of the pressure changes, although we predicted that the delay would be minimal. The respiratory condition was primarily determined by the anesthesiologist, depending on the patient's condition. Because it was difficult to adjust the delay time frequently referring to the respiratory rate, fixed delay times of 500 and and 100 ms for near-real-time MR images and temperature increase maps, respectively, were utilized and the results were deemed satisfactory.

With this triggering, the images were clear and their positions were quite stationary. For easy detection of the location, images in the sagittal plane are shown in Figure 2. Usually, images in the axial plane were used for image guidance. Without respiratory triggering, the target was frequently missed, depending on the respiratory phase. For tumors 20–30 mm in diameter, movements of 15–23 mm were substantial. With respiratory triggering, however, targeting of the tumor became much easier. With this option, the update time of the near-real-time images was reduced, depending on the respiratory rate. However, smaller numbers of clear images worked better than larger numbers of blurred ones. This function has been mainly utilized for needle tracking in cases with small-sized tumors.

Using this technique, temperature changes during microwave ablation could be monitored without suspending the artificial ventilation. Previously, respiration was suspended for a base-line image, then the patient was hyperventilated. Thereafter, respiratory suspension and hyperventilation were alternately repeated during the 3-minute microwave thermocoagulation. Now, with triggering, it is not necessary for the anesthesiologist to stop the breathing for MR image acquisition. Triggering made this procedure both easy and safe. In addition, the preparation time for temperature monitoring could be reduced. Various factors other than the respiratory movement, such as the movements of both the surgeons and surgical instruments, and drifts of the static magnetic field, affected the temperature calculation. A strict comparison between the temperature increase maps and respiratory suspension and respiratory triggering is difficult to achieve, but we have completely moved to respiratory triggering for MR temperature monitoring with satisfactory results.

In conclusion, respiratory triggering specifically designed for MR-guided thermocoagulation therapy under general anesthesia was found to be useful for targeting with near-real-time MR images and MR temperature monitoring in MR-guided microwave ablation of liver tumors.

References

1. Schenck JF, Jolesz FA, Roemer PB (1995) Superconducting open-configuration MR imaging system for image-guided therapy. Radiology 195:805–814
2. Tabuse K (1979) A new operative procedure of hepatic surgery using a microwave tissue coagulator. Arch Jpn Chir 48:160–172
3. Hamazoe R, Hirooka Y, Ohtani S (1995) Intraoperative tissue coagulation as treatment for patients with nonresectable hepatocellular carcinoma. Cancer 75:94–800
4. Seki T, Wakabayashi M, Nakagawa T (1994) Ultrasonically guided percutaneous microwave coagulation therapy for small hepatocellular carcinoma. Cancer 74:817–825
5. Ido K, Isoda N, Kawamoto C (1997) Laparoscopic microwave coagulation for solitary hepatocellular carcinoma performed under laparoscopic ultrasonography. Gastrointest Endosc 45:415–420
6. Morikawa S, Inubushi T, Kurumi Y (2001) Feasibility of microwave ablation for MR-guided interstitial thermal therapy: an experimental study using 2T MR system. Jpn J Magn Reson Med 21:79–84
7. Morikawa S, Inubushi T, Kurumi Y (2002) MR-guided microwave thermocoagulation therapy of liver tumors: initial clinical experiences using a 0.5 T open MR system. J Magn Reson Imaging 16:576–583
8. Morikawa S, Inubushi T, Kurumi Y (2003) New assistive devices for MR-guided microwave thermocoagulation of liver tumors. Acad Radiol 10:80–188
9. De Poorter J, De Wagter C, De Deene Y (1995) Noninvasive MRI thermometry with the proton resonance frequency (PRF) method: in vivo results in human muscle. Magn Reson Med 33:74–81
10. Quesson B, de Zwart JA, Moonen CTW (2000) Magnetic resonance temperature imaging for guidance of thermotherapy. J Magn Reson Imaging 12:525–533
11. Runge VM, Clanton JA, Partain CL (1984) Respiratory gating in magnetic resonance imaging at 0.5 Tesla. Radiology 151:521–523
12. Jhooti P, Wiesmann F, Taylor AM (1998) Hybrid ordered phase encoding (HOPE): an improved approach for respiratory artifact reduction. J Magn Reson Imaging 8:968–980
13. Ehman RL, Felmlee JP (1989) Adaptive technique for high-definition MR imaging of moving structures. Radiology 173:255–263
14. Sachs TS, Meyer CH, Irarrazabal P (1995) The diminishing variance algorithm for real-time reduction of motion artifacts in MRI. Magn Reson Med 34:412–422